Domain Structure and Conformation of Histidine−Proline-Rich Glycoprotein[†,‡]

Dorin-Bogdan Borza,[§] Fred M. Tatum,[||] and William T. Morgan*[,§]

Division of Molecular Biology and Biochemistry, School of Biological Sciences, University of Missouri−Kansas City, Kansas City, Missouri 64110, and National Animal Disease Center, United States Department of Agriculture, Ames, Iowa 50010

Received August 30, 1995; Revised Manuscript Received October 31, 1995[⊗]

ABSTRACT: The complete primary structure of rabbit plasma histidine−proline-rich glycoprotein (HPRG), also known as histidine-rich glycoprotein, was determined by a combination of cDNA and peptide sequencing. Limited proteolysis with plasmin yielded three disulfide-linked fragments that were further purified. Reduction of the disulfide bonds with dithiothreitol under nondenaturing conditions releases the central, histidine−proline-rich domain, which contains 15 tandem repeats of the pentapeptide [H/P]-[H/P]PHG. The N-terminal fragment (295 amino acids), consisting of two cystatin-like modules, is bound to the proline-rich C-terminal fragment (105 amino acids) via a buried disulfide bond whose reduction requires prior denaturation. Far-UV circular dichroism spectra revealed β-sheet with some α-helix, polyproline-II helix, and random coil in the secondary structure of the N-terminal, central, and C-terminal domains, respectively. The modular architecture of HPRG suggests that it may have several independent binding sites and that its biological role may be to bring two or more ligands together. The histidine−proline-rich domain, which contains 34 of the 53 histidine residues of HPRG, binds heparin and has an isoelectric point of 7.15 and a relatively high apparent pK_a (7.0) of its histidine residues, and thus it probably mediates the interaction between HPRG and heparin, which is strikingly sensitive to pH in the range 7.0−7.4 [Peterson *et al*. (1987) *J. Biol. Chem. 262*, 7567−7574]. Solvent perturbation and second-derivative UV spectroscopy of HPRG revealed changes in the environment of tryptophan residues upon lowering the pH. This transition had a midpoint at pH 6.0 and required the disulfide bond bridging the histidine−proline-rich domain to the N/C fragment. The data are consistent with the mutual repulsion of protonated histidine residues in the histidine−proline-rich region causing a conformational change transmitted to the rest of the molecule *via* the disulfide bond.

Histidine−proline-rich glycoprotein[1] (HPRG)[2] is a plasma glycoprotein belonging to the cystatin superfamily (Koide & Odani, 1987), along with α_2HS glycoprotein and kininogen. The most salient feature of HPRG, reflected in its name, is a high content of both histidine and proline. Although the physiological role (or roles) of HPRG has not been unequivocally established, several biological functions have been suggested on the basis of its *in vitro* ligand binding properties. The sundry assortment of HPRG ligands can be classified in three broad categories: (a) small ligands, such as heme and transition series metals (Morgan, 1978); (b) ligands belonging to the hemostatic coagulation−fibrinolysis system, including heparin (Lijnen *et al*., 1983), plasminogen (Lijnen *et al*., 1980), fibrinogen (Leung *et al*., 1984), and thrombospondin (Leung *et al*., 1984); and (c) components of the immune system, such as vitronectin (Chang *et al*., 1992b), T-cells (Saigo *et al*., 1989), and macrophages (Chang *et al*., 1992a).

Until now, only the full sequence of human HPRG (Koide *et al*., 1986) and partial sequence data for the bovine protein (Sorensen *et al*., 1993) have been reported. Here we report the primary structure of rabbit plasma HPRG based on its cDNA sequence. Rabbit HPRG shares many properties of the human protein, including binding of heme and metals (Morgan, 1985), plasminogen (Saez *et al*., 1995), and heparin (Peterson *et al*., 1987). In this work, we used the rabbit protein since its higher serum concentration (900 mg/L versus 125 mg/L in human plasma) facilitates isolation of large amounts of intact protein, and it has conveniently situated plasmin cleavage sites that allow the isolation and characterization of HPRG structural domains. The analysis of HPRG regions structurally conserved across species should help identify the residues important for its biological function, and the purification of HPRG domains enables more detailed study of structure−function relationships, as well as the mapping of HPRG binding sites for its various ligands.

Rabbit plasma HPRG contains 53 histidine residues, of which 34 are located in the histidine−proline-rich central region. Since histidine titrates in the physiological pH range, this domain can accumulate a large number of positive charges upon lowering the pH, with possible consequences to both the structure and function of HPRG. A previous

[†] This work was supported in part by a grant (HL-37570) from the U.S. Public Health Service, National Institutes of Health.

[‡] The nucleotide sequence reported in this paper has been submitted to the GenBank/EMBL Data Bank under Accession Number U32189.

* To whom correspondence should be addressed.

[§] University of Missouri−Kansas City.

[||] USDA.

[⊗] Abstract published in *Advance ACS Abstracts*, January 15, 1996.

[1] "Histidine−proline-rich glycoprotein" is used rather than the former name "histidine-rich glycoprotein" since the C-terminal half of the protein is rich in both histidine and proline. Furthermore, the revised term avoids confusion with the *Plasmodium*-secreted histidine-rich protein and the salivary histidine-rich polypeptides.

[2] Abbreviations: HPRG, histidine−proline-rich glycoprotein; RCAM, reduced and carboxamidomethylated; PRCAM, partially reduced and carboxamidomethylated; DTT, dithiothreitol; SDS, sodium dodecyl sulfate; EDTA, ethylenediaminetetraacetic acid; DMSO, dimethyl sulfoxide; DEAE, diethylaminoethyl; PAGE, polyacrylamide gel electrophoresis; IEF, isoelectric focusing; UV, ultraviolet; CD, circular dichroism; M_r, relative molecular mass ("molecular weight"); $s_{20,w}$, sedimentation coefficient under standard conditions.

0006-2960/96/0435-1925$12.00/0

study has shown that the interaction between HPRG and heparin is strikingly pH-sensitive (Peterson *et al*., 1987). Here, we used several physicochemical methods to examine the properties of rabbit HPRG and its domains, as well as the effects of protonation of the histidine side chains on the conformation of the protein.

MATERIALS AND METHODS

Reagents. Rabbit HPRG was isolated from serum (Pel-Freeze, Rogers, AR) using the protocol described for hemopexin purification (Morgan *et al*., 1993), except that the sodium chloride gradient on the second (diethyl-aminoethyl)cellulose (DE-52, Whatman) column was further extended to obtain HPRG. HPRG elutes at 0.15 M sodium chloride, and it forms the first peak following the hemopexin fractions. The resulting fractions were dialyzed against 5 mM phosphate buffer (pH 7.2), concentrated by ultrafiltration, and stored in aliquots at −20 °C. Approximately 600 mg of HPRG was obtained from 2 L of serum (*ca*. 30% yield). The isolated protein migrated as a single band with an apparent M_r near 90 000 on SDS−PAGE under reducing conditions. Partially reduced HPRG (PRCAM-HPRG) was prepared by incubation with 25 mM DTT in 0.1 M phosphate buffer (pH 7.3) containing 5 mM EDTA. The reaction was allowed to proceed for 60 min on ice in the dark, and then the free sulfhydryl groups were alkylated with 55 mM iodoacetamide (Research Organics, Cleveland, OH) for 30 min. The reaction mixture was then desalted by gel filtration. Fully reduced HPRG (RCAM-HPRG) was similarly prepared, except that 3 M guanidine hydrochloride was incorporated in the reduction buffer.

Plasminogen was isolated as described (Castellino & Powell, 1981) from human plasma and immobilized on BrCN-activated Sepharose-4B (Pharmacia) according to the manufacturer's protocol. The immobilized plasminogen (7 mg/mL of gel) was activated by incubation overnight with urokinase (Calbiochem) at 4 °C in 50 mM sodium phosphate (pH 7.3) containing 100 mM sodium chloride. Heparin (porcine intestinal mucosa, grade I−A) was from Sigma.

HPRG Domain Isolation. Rabbit HPRG (10 mg/mL in 0.1 M sodium phosphate buffer, pH 7.4) was partially proteolyzed by stirring with plasmin−Sepharose (1 mL of gel for 15 mL of HPRG solution) for 4 h at 4 °C. The optimal digestion time was determined using SDS−PAGE under reducing conditions of aliquots taken at different times. Partial reduction and carboxamidomethylation of plasmin-clipped HPRG were achieved as described above for HPRG. The reaction mixture was dialyzed extensively against 20 mM sodium phosphate (pH 7.3) and applied to a DEAE-cellulose column equilibrated in the same buffer. A histidine−proline-rich peptide, later identified as the central domain of HPRG, passed through the column unretarded. The column was then washed with 30 mM sodium phosphate (pH 6.3) to remove undigested HPRG and eluted with a sodium chloride gradient (0−200 mM) to yield a fragment termed N/C, which is composed of the disulfide-linked N- and C-terminal domains of HPRG. The N/C fragment was reduced with DTT and alkylated as described above, incorporating 3 M guanidine hydrochloride in the reduction buffer. After desalting, the mixture was applied to a Blue-Sepharose (Pharmacia) column equilibrated with 20 mM sodium phosphate (pH 7.3). The N-terminal domain was eluted with 0.5 M sodium chloride in the same buffer. The C-terminal domain was eluted with 0.5 M sodium chloride in 50 mM Tris buffer (pH 8.8). All HPRG domains thus obtained were additionally purified by gel filtration on Ultrogel AcA-44 (LKB), and aliquots were stored at −20 °C in 5 mM phosphate buffer (pH 7.2).

N-Terminal amino acid sequences of HPRG and the HPRG-derived domains were determined after electrophoretic transfer to Immobilon-P (Millipore) by Edman microsequencing using an ABI 477A protein sequencer in the Molecular Biology Core Facility, School of Biological Sciences, University of Missouri−Kansas City. Each sample was sequenced for at least 8 cycles. For amino acid analyses, samples blotted onto Immobilon-P were hydrolyzed with HCl at 105 °C for 22 h and analyzed with an ABI 420A amino acid analyzer by the Core Facility.

Molecular Cloning of Rabbit HPRG cDNA. A rabbit liver cDNA λgt11 expression library (*ca*. 1×10^6 members) from Clontech was screened with a mixture of monoclonal antibodies to rabbit HPRG followed by alkaline phosphatase-conjugated goat anti-mouse IgG (Bio-Rad). The positive plaques for HPRG were recovered and purified by homogeneity. Phage DNA was prepared by the plate lysate method (Sambrook *et al*., 1989) and a slight modification of the immunoprecipitation procedure using "Lambdasorb" phage adsorbent (Promega). Recombinant DNA for sequencing was obtained as described (Struhl, 1985). The DNA (usually 10−15 μg) was digested with *Eco*RI (Gibco−BRL, 10 units) for 60 min at 37 °C. The restricted DNA was electrophoresed in 1.0% low-melting-point agarose (Bio-Rad) in Tris−acetate−EDTA buffer. The cDNA insert was located with ethidium bromide, excised, and ligated in the melted agar at 70 °C into the sequencing vector pUC118 using T4 ligase (Gibco−BRL). The 5′ and 3′ ends of each cDNA insert were sequenced by the dideoxy method (Sanger *et al*., 1980) using ^{35}S-dATP (DuPont−New England Nuclear), Sequenase II kits (U.S. Biochemical Corp.), and buffer-gradient gels containing 0.5−5X Tris−borate−EDTA (Biggin *et al*., 1983). Comparisons with the known human HPRG sequence and portions of the rabbit HPRG sequence obtained by Edman microsequencing facilitated sequence alignments. Each portion of DNA was sequenced at least twice. Sequence data were managed and analyzed using the PC/Gene package (Intelligenetics).

Physicochemical Studies. The concentrations of HPRG and its domains were measured by the tyrosine−tyrosinate difference spectrum method, using the number of tyrosine residues deduced from the sequence and a difference extinction coefficient, $\Delta\epsilon$, of 2.33 mM^{-1} cm^{-1} per tyrosine at 295 nm (Donovan, 1973). For rabbit HPRG, which contains 10 tyrosine residues, this method yields a molar extinction coefficient of 36.5 mM^{-1} cm^{-1} at 278 nm. Since the histidine−proline-rich domain does not contain tyrosine, its molar extinction coefficient (340 mM^{-1} cm^{-1} at 220 nm) was obtained by titration of the histidine residues with diethyl pyrocarbonate (Miles, 1977).

SDS−PAGE was carried out on 12% acrylamide gels using a discontinuous buffer (Laemmli, 1970). Protein bands on the gels were visualized by staining with Coomassie Brilliant Blue G-250. Isoelectric focusing and electrophoretic titration curves were performed in a Pharmacia Phast System electrophoresis apparatus, following the manufacturer's instructions. Precast IEF gels (Pharmacia) with the pH range

5−8 for isoelectric focusing and 3−9 for titration curves were used. The p*I* values were determined from a calibration curve using the p*I* values of standard proteins.

UV spectra were obtained on a diode-array Aminco 3000 SLM spectrophotometer (Milton-Roy) at 0.35-nm resolution using at least 10 accumulations. The second-derivative spectra were computed by the Savitski−Golay algorithm using a 9-point smoothing interval. Difference spectra were obtained in tandem quartz cuvettes. Either ethylene glycol (Fisher Scientific) or DMSO (Sigma) at a final concentration of 20% was used as perturbant. Fluorescence spectra were recorded at 25 °C in 10 mM sodium phosphate (pH 7.2) containing 100 mM sodium chloride with an SLM Aminco-Bowman Series 2 luminescence spectrometer.

Far-UV (245−185 nm) and near-UV (320−240 nm) CD spectra were recorded at room temperature at 50 nm/min on a Jasco J-720 spectropolarimeter, using the auto slit width program and a 2-s time constant. Cylindrical quartz cuvettes with a 1-mm path length for the far-UV and 10-mm path length for the near-UV region were used. At least 10 scans were averaged for each measurement, and the resulting spectra were normalized to molar ellipticities using the known concentrations after averaging and smoothing using Jasco Series 700 software.

Sedimentation velocity experiments were performed with a Beckman XL-A analytical ultracentrifuge at speeds of 40 000 (55 000 rpm for the histidine−proline-rich domain), using an An-60 rotor and 12-mm double sector centerpieces, at a constant temperature of 20 or 25 °C. The protein samples were dissolved in 10 mM sodium phosphate buffer containing 0.15 M sodium chloride and 0.25 mM EDTA; the pH was 7.2 unless otherwise indicated. A relatively low protein concentration (0.5−1 mg/mL for HPRG, 0.25 mg/mL for the histidine−proline-rich domain) and moderate ionic strength were used to minimize primary charge effects when working at the different pH values. To facilitate direct comparison and minimize the influence of systematic errors (such as variations in the rotor temperature), samples differing only in their pH values were analyzed in parallel in the same centrifuge run since up to three samples can be fitted in the An-60 rotor. Absorbance *vs* radius data were collected by continuous scan at 233 nm and stored digitally; this wavelength was used since the histidine−proline-rich domain lacks aromatic residues and to achieve sensitivity at low protein concentration. The apparent sedimentation coefficients and their 95% confidence intervals, computed by analyzing the sedimentation profiles with the program Svedberg (Philo, 1994), were corrected for the density and viscosity of buffer as described (Laue *et al*., 1992) to yield the sedimentation coefficients under standard conditions.

RESULTS

cDNA Sequence and Primary Structure of Rabbit HPRG. The sequence of cloned rabbit HPRG cDNA is shown in Figure 1 together with the deduced amino acid sequence. Although the cDNA lacks the start codon, the reading frame was identified by comparison with the N-terminal amino acids of mature rabbit HPRG obtained by peptide sequencing (NH_2-LTPTDXKTTKPLAEK). The mature protein has 518 amino acids and a molecular weight calculated from the sequence of 58 016. The overall architecture of rabbit HPRG is similar to that described for the human protein (Koide *et al*., 1986): the N-terminal half of the molecule has an unbiased amino acid composition and contains two modules homologous to cystatin, while the C-terminal half consists of a histidine−proline-rich pentapeptide repeat region sandwiched between proline-rich regions. Rabbit HPRG contains 17.5% carbohydrate (Morgan, 1985), which would increase the molecular weight of the protein to about 70 000. There are five potential N-glycosylation sites with the consensus sequence Asn-X-Ser/Thr (Asn-107, Asn-184, Asn-232, Asn-302, and Asn-477) and three possible O-glycosylation sites (Thr-8, Thr-247, and Ser-274) predicted by a neutral network pattern recognition algorithm (Hansen *et al*., 1995).

The alignment of rabbit HPRG with the human (63.5% identity, 68.6% similarity) and bovine (58.8% identity, 65.3% similarity) proteins is shown in Figure 2. The highest homology occurs at the amino and carboxyl termini. However, the apparent lower homology over the histidine−proline-rich region is primarily due to the substitution of some histidine residues for proline in the rabbit protein (a single base change). Human HPRG contains 10 tandem repeats of the sequence HHPHG, and the rabbit HPRG contains 15 repeats of HHPHG (2 times), HPPHG (6 times), or PPPHG (7 times). Thus, the consensus sequence that appears to be a hallmark or histidine−proline-rich glycoproteins is [H/P][H/P]PHG.

Rabbit HPRG Domains. Plasmin cuts at the carboxyl side of exposed lysine or arginine residues, and intact protein domains can be obtained by controlling the digestion time. Plasmin cleavage of HPRG produces three disulfide-linked fragments (Morgan, 1985), with apparent molecular masses of 40, 30, and 20 kDa by reducing SDS−PAGE, which migrate as a single band under nonreducing conditions. N-Terminal amino acid sequencing of the proteolytic fragments and comparison with the primary structure of HPRG deduced from the cDNA indicated that Arg-295 and Lys-413 are the main plasmin cleavage sites, enabling the assignments shown in Table 1. Figure 3 shows a schematic diagram of the HPRG domains. The 40-kDa fragment[3] has the same N-terminal sequence as the intact protein and thus represents the N-terminal half of the molecule. The 30-kDa fragment encompasses the histidine−proline-rich region (residues 296−413), and the 20-kDa fragment represents the C-terminal 105 amino acids. Longer digestion time allows further cleavage of the 20-kDa C-terminal domain into a 6-kDa fragment (NH_2-XGPQDL) and a previously described (Morgan *et al*., 1989) 15-kDa fragment (NH_2-GHFPFH). As Table 1 shows, all HPRG domains migrate in SDS−PAGE at higher apparent molecular masses than those deduced from their sequences. This is expected for the N-terminal domain in the view of its six putative glycosylation sites (see Figure 2), but for the histidine−proline-rich and C-terminal domains, it is likely that the discrepancy is caused by their high proline content.

There is a good agreement between the experimental amino acid composition of HPRG fragments [data not shown; see Morgan (1985)] and that calculated from the predicted domain boundaries, except that the N-terminal fragment contains less proline than expected. This may be explained by a secondary plasmin cleavage at Lys-242, Arg-251, or Lys-261, which would remove the proline-rich peptide

[3] The HPRG domains are referred to by their apparent molecular masses, as obtained from reducing SDS−PAGE (see Figure 4).

```
GCGCCACACTGCAGTGTTCGTGGGCTTTGACTCCCACTGACTGCAAAACTACCAAGCCCTTGGCTGAGAAAGCTCT -76
  AlaThrLeuGlnCysSerTrpAlaLeuThrProThrAspCysLysThrThrLysProLeuAlaGluLysAlaLe

AGACCTGATCAATAAATGGCGACGGGATGGCTACCTTTTCCAGTTGCTGCGAGTCGCTGATGCCCACTTGGACGGA -152
uAspLeuIleAsnLysTrpArgArgAspGlyTyrLeuPheGlnLeuLeuArgValAlaAspAlaHisLeuAspGly

GCGGAATCTGCCACTGTCTACTATTTAGTCTTAGATGTGAAAGAGACTGACTGTTCAGTGCTATCCAGGAAACACT -228
AlaGluSerAlaThrValTyrTyrLeuValLeuAspValLysGluThrAspCysSerValLeuSerArgLysHisT

GGGAAGACTGTGACCCAGATCTTACTAAACGTCCATCTCTTGACGTGATTGGGCAATGTAAGGTGATAGCTACCAG -304
rpGluAspCysAspProAspLeuThrLysArgProSerLeuAspValIleGlyGlnCysLysValIleAlaThrAr

ATATTCGGATGAATATCAGACTCTAAGATTGAATGACTTTAACTGCACCACGAGTTCCGTCTCTTCAGCCCTGGCC -380
gTyrSerAspGluTyrGlnThrLeuArgLeuAsnAspPheAsnCysThrThrSerSerValSerSerAlaLeuAla

AACACTAAAGACAGTCCTGTTCTCTTTGATTTCATCGAGGACACGGAGCCCTTCAGAAAATCCGCGGACAAAGCCC -456
AsnThrLysAspSerProValLeuPheAspPheIleGluAspThrGluProPheArgLysSerAlaAspLysAlaL

TGGAGGTGTACAAAAGTGAAAGCGAGGCGTATGCCTCTTTCAGAGTGGACCGGGTAGAGAGAGTCACAAGGGTGAA -532
euGluValTyrLysSerGluSerGluAlaTyrAlaSerPheArgValAspArgValGluArgValThrArgValLy

AGGAGGAGAGAGAACCAATTACTATGTGGACTTCTCCGTGAGGAACTGCTCCAGGTCTCACTTCCACAGACACCCC -608
sGlyGlyGluArgThrAsnTyrTyrValAspPheSerValArgAsnCysSerArgSerHisPheHisArgHisPro

GCCTTTGGGTTCTGCAGAGCAGATCTGTCCTTTGATGTAGAAGCCTCGAACTTGGAAAACCCAGAAGACGTTATTA -684
AlaPheGlyPheCysArgAlaAspLeuSerPheAspValGluAlaSerAsnLeuGluAsnProGluAspValIleI

TAAGCTGTGAAGTCTTTAACTTTGAGGAACATGGAAACATCAGTGGTTTTCGACCCCATTTGGGCAAGACTCCACT -760
leSerCysGluValPheAsnPheGluGluHisGlyAsnIleSerGlyPheArgProHisLeuGlyLysThrProLe

TGGGACTGATGGATCCAGAGATCATCATCATCCCCACAAGCCACATAAGTTTGGATGCCCACCTCCCCAAGAAGGG -836
uGlyThrAspGlySerArgAspHisHisHisProHisLysProHisLysPheGlyCysProProProGlnGluGly

GAAGATTTCTCGGAAGGACCACCACTTCAAGGTGGAACCCCCCCACTCTCCCCCCCCTTCAGGCCAAGATGTCGTC -912
GluAspPheSerGluGlyProProLeuGlnGlyGlyThrProProLeuSerProProPheArgProArgCysArgH

ATCGCCCTTTTGGCACCAATGAAACCCATCGGTTCCCTCATCATCGAATTTCAGTGAACATCATCCATAGGCCCCC -988
isArgProPheGlyThrAsnGluThrHisArgPheProHisHisArgIleSerValAsnIleIleHisArgProPr

TCCCCATGGACATCACCCCCATGGGCCCCCTCCCCATGGACATCACCCCCATGGGCCCCCTCCCCATGGACATCCT -1064
oProHisGlyHisHisProHisGlyProProProHisGlyHisHisProHisGlyProProProHisGlyHisPro

CCTCATGGACCCCCTCCCCGACATCCTCCCCATGGGCCTCCTCCCCATGGACATCCCCCCCATGGACCCCCTCCCC -1140
ProHisGlyProProProArgHisProProHisGlyProProProHisGlyHisProProHisGlyProProProH

ATGGACATCCTCCTCATGGACCCCCTCCCCATGGACATCCTCCCCATGGGCCCCCTCCCCATGGACATCCTCCCCA -1216
isGlyHisProProHisGlyProProProHisGlyHisProProHisGlyProProProHisGlyHisProProHi

TGGCCATGGTTTCCATGACCATGGACCCTGTGACCCACCATCCCATAAAGAAGGTCCCCAAGACCTCCATCAGCAT -1292
sGlyHisGlyPheHisAspHisGlyProCysAspProProSerHisLysGluGlyProGlnAspLeuHisGlnHis

GCCATGGGACCACCACCTAAGCACCCAGGAAAGAGAGGTCCAGGTAAAGGACACTTTCCCTTCCACTGGAGAAGAA -1368
AlaMetGlyProProProLysHisProGlyLysArgGlyProGlyLysGlyHisPheProPheHisTrpArgArgI

TTGGGTCTGTTTACCAACTGCCCCCACTGCAGAAAGGTGAAGTCCTTCCCCTTCCCGAAGCCAATTTTCCCCAGCT -1444
leGlySerValTyrGlnLeuProProLeuGlnLysGlyGluValLeuProLeuProGluAlaAsnPheProGlnLe

TCTCTTGCGGAACCACACCCACCCTCTAAAGCCCGAGATCCAGCCCTTCCCTCAGGTAGCCTCTGAGCGCTGTCCA -1520
uLeuLeuArgAsnHisThrHisProLeuLysProGluIleGlnProPheProGlnValAlaSerGluArgCysPro

GAGGAGTTCAATGGTGAGTTTGCACAACTCTCCAAGTTTTTCCCATCTACATTTCCAAAATGAAATCTGATTTCCT -1596
GluGluPheAsnGlyGluPheAlaGlnLeuSerLysPhePheProSerThrPheProLysSTOP

TGATGGGNAACAATGAATGATATTCTGTATTAGCACCATAAATAAAATGTGGCCATGATGAATGCAAAAAAAAAAAA-1673
```

FIGURE 1: Nucleotide and deduced amino acid sequence of cloned rabbit HPRG cDNA. The NH_2-terminal amino acid of the mature protein, identified by peptide sequencing, is double-underlined. The cloned cDNA encompasses the last eight residues of the signal peptide (in italics) and the full 518 amino acid sequence of the mature protein. The stop codon, TGA, is followed by a 78-nucleotide 3′-untranslated region before the poly(A) tail. The polyadenylation signal is underlined.

upstream of these residues. Indeed, the N-terminal fragment can be resolved by reducing SDS−PAGE into two bands differing by about 3 kDa, and the relative intensity of the lower MW band increases with digestion time. The second derivative of the near-UV spectra of HPRG and its domains (data not shown) are also consistent with the predicted content of aromatic acids of each species (Table 1).

Treating the clipped HPRG with DTT under nondenaturing conditions cleaves the disulfide bond linking the histidine−proline-rich domain to the rest of the molecule. This domain

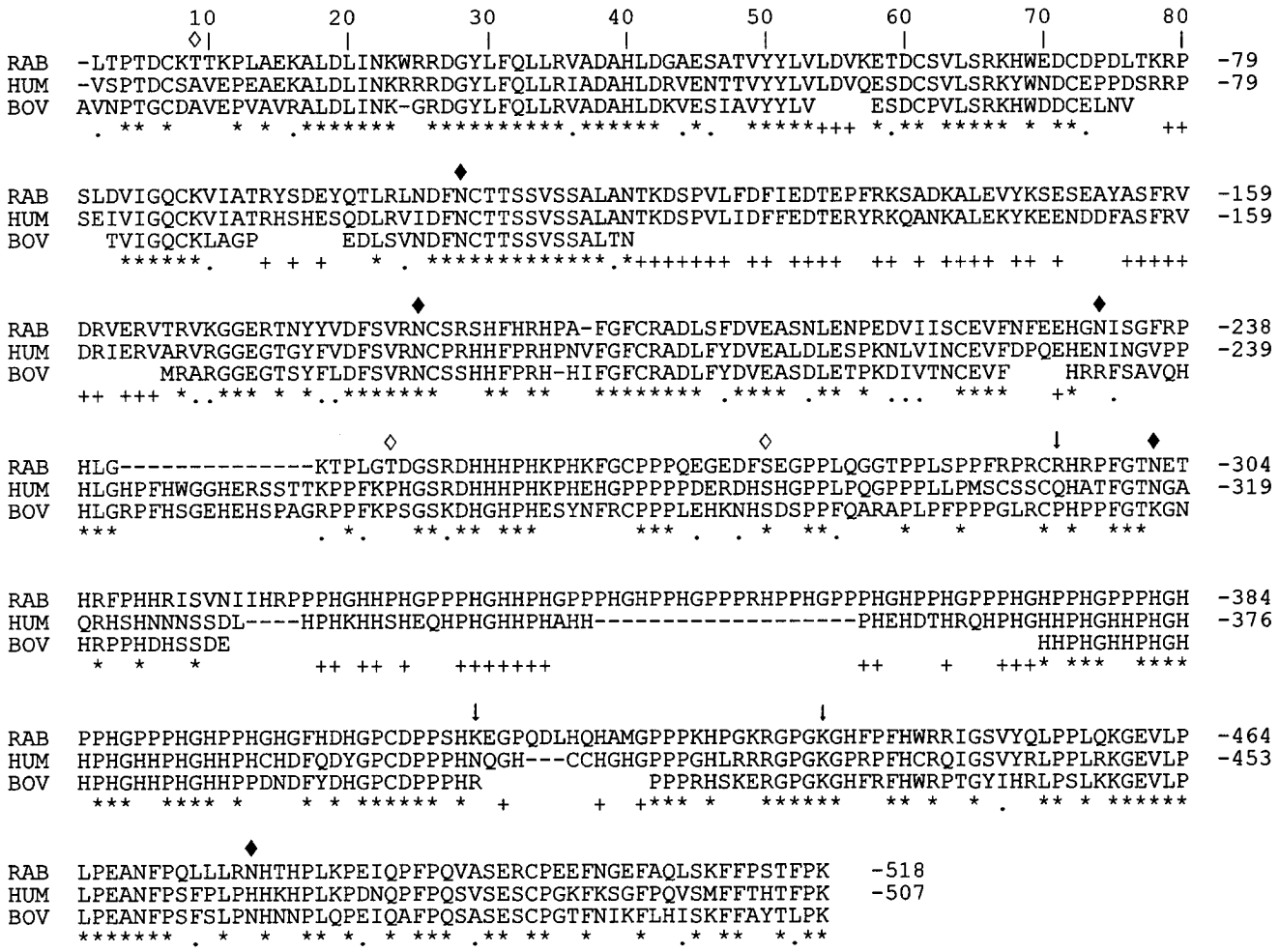

FIGURE 2: Comparison of the amino acid sequences of rabbit, human, and bovine HPRG. The alignment was computed using the program CLUSTALL of the PC/Gene suite. Gaps in the alignment are symbolized by a dash. Identical amino acids are indicated by a star and similar amino acids by a dot. A plut sign represents identical residues in the rabbit and human sequences where no data were available for the bovine sequence (blank regions in the alignment). The putative N- and O-glycosylation sites of rabbit HPRG are shown as closed and open diamonds, respectively. The major and minor plasmin cleavage sites are denoted by thick or thin arrows, respectively.

Table 1: Properties of HPRG and Its Domains

	HPRG	N/C fragment	N-terminal domain	His−Pro-rich domain	C-terminal domain
Apparent M_r[a] (×1000)	90	65	45	30	20
N-terminal sequence[a]	LTPTDXKTTKP	N/A[d]	LTPTDXKTTKP	XXPFGTXETH	EGPQXLXQ
amino acid residues[b]	1−518	1−295, 414−518	1−295	296−413	414−518
calculated MW[c] (×1000)	58	45.3	33.4	12.7	11.9
putative N- and O-glycosylation sites[c]	5 Asn; 2 Thr, 1 Ser	4 Asn; 2 Thr, 1 Ser	3 Asn; 2 Thr, 1 Ser	1 Asn	1 Asn
aromatic amino acids (Trp:Tyr:Phe)[c]	3:10:29	3:10:26	2:9:17	0:0:3	1:1:9
$s_{20,w}$[a] (10^{-13} s)	4.44	3.79	N/D[d]	1.53	N/D[d]
isoelectric pH (p*I*)[a]	6.45	5.6−5.8	N/D[d]	7.15	N/D[d]

[a] Experimentally determined, as described in text. [b] Deduced from the N-terminal amino acid sequence of the HPRG domains. [c] Inferred from the sequence. [d] N/A, not applicable; N/D, not determined.

can then be easily separated by ion-exchange chromatography on DEAE-cellulose. The N/C fragment migrates as a single, broad band with an apparent molecular mass of 60 kDa in nonreducing SDS−PAGE. The reduction of the disulfide bridge between the N- and C-terminal domains requires prior denaturation, suggesting that this bond is buried within a hydrophobic contact area. Even after reduction, separation of these two domains by ion-exchange chromatography is difficult, presumably because of residual hydrophobic interactions. Consistent with this view, the location at 248 nm of the emission maximum in the fluorescence spectrum of the C-terminal domain denotes solvent exposure of Trp-445; in contrast, the fluorescence emission maxima of HRPG, N/C fragment, and N-terminal domains are located at 239−240 nm, indicating a moderately hydrophobic tryptophan environment. We found that Blue-Sepharose, a chromatographic medium which exhibits both electrostatic and hydrophobic interactions, was the most effective in the purification of the N- and C-terminal domains. A reducing SDS−PAGE profile of the domains of HPRG thus obtained is shown in Figure 4.

Structure of HPRG Domains. Near-UV circular dichroism was used to compare the tertiary structure of HPRG and its derivatives. CD spectra in this region arise from the contribution of aromatic residues and disulfide bonds and, although difficult to interpret quantitatively, can serve as

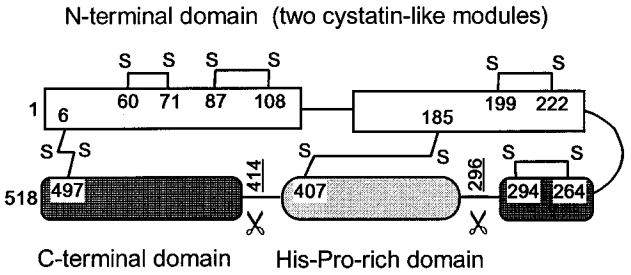

FIGURE 3: Schematic diagram of the domain structure of rabbit HPRG. The N-terminal half of HPRG consists of two cystatin-like modules (white). The C-terminal half of the molecule consists of a histidine−proline-rich pentapeptide repeat region (light gray) sandwiched between two proline-rich regions (dark gray). The scissors symbol indicates the major plasmin cleavage sites. The pattern of disulfide bonds in the rabbit HPRG was inferred on the basis of the homology to the bovine HPRG, since all 12 cysteine residues are conserved between the two species.

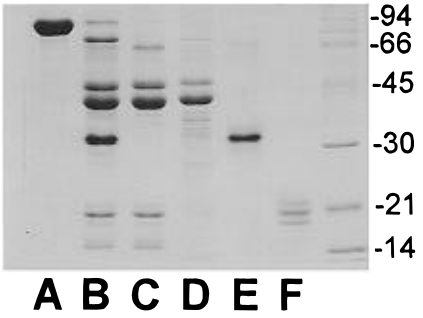

FIGURE 4: Reducing SDS−PAGE of rabbit HPRG and its domains. HPRG (0.1 nmol) and HPRG domains (0.2 nmol) were run on 12% PAGE in the presence of SDS and DTT and then stained with Coomassie Brilliant Blue. Shown are lane *A*, HPRG; lane *B*, clipped HPRG; lane *C*, the N/C fragment; lane *D*, the N-terminal domain; lane *E*, the histidine−proline-rich domain; and lane *F*, the C-terminal domain.

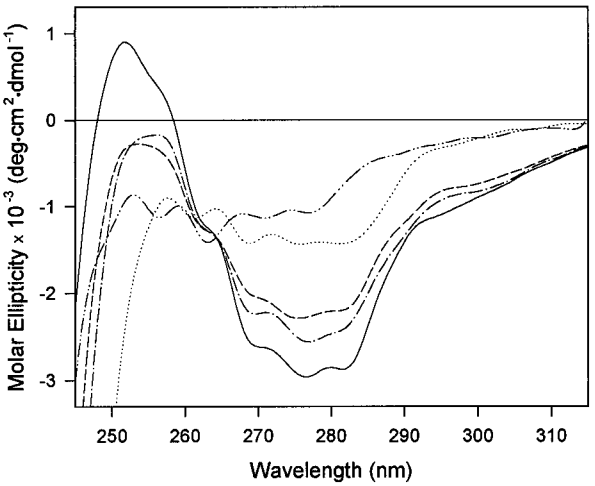

FIGURE 5: Near-UV CD spectra of HPRG and its domains. The spectra were obtained in 10 mM phosphate buffer, pH 7.2, and converted to molar ellipticities (deg·cm^2·dmol^{-1}) after averaging and smoothing. Shown are HPRG (—), N/C fragment (− − −), PRCAM-HPRG (− · −), RCAM-HPRG (− ·· −), and HPRG in the presence of 3 M guanidine hydrochloride (···).

"fingerprints" for the native state of a protein. The spectrum of native HPRG displays a positive band at 252 nm and a broad negative band with fine structure centered at 277 nm (Figure 5). The N/C fragment exhibits a spectrum similar to that of the native HPRG above 260 nm, but the intensity of the positive peak at 252 nm is decreased. Since the spectrum of the N/C fragment is virtually identical to that

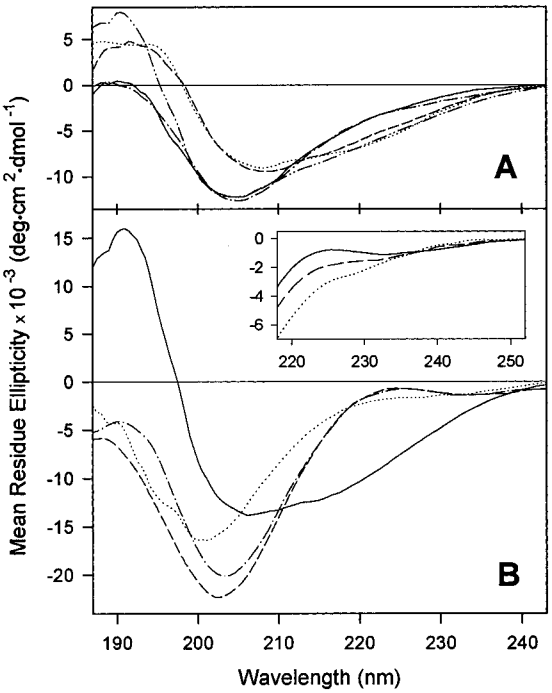

FIGURE 6: Far-UV CD spectra of the HPRG and its domains. The spectra were obtained in 5 mM phosphate buffer, pH 7.2, and converted to mean residue ellipticity (deg·cm^2·dmol^{-1}) after averaging and smoothing. Panel *A*: HPRG (—), simulated HPRG (− · −), N/C fragment (− − −), simulated N/C fragment (− ·· −), and fetuin (···). Simulated spectra represent the best fit obtained by addition of the spectra of the component domains (see text). Panel *B*: N-Terminal domain (—), C-terminal domain (···), histidine−proline-rich domain (− − −), and histidine−proline-rich domain in the presence of excess heparin (− · −). The latter spectrum was corrected for the small contribution of the heparin. *Inset:* Histidine−proline-rich domain in the absence (—) and in the presence of 2.7 M (− − −) and 5.4 M (···) calcium chloride.

of PRCAM-HPRG, it is likely that the partial reduction of disulfide bonds and not the removal of the histidine−proline-rich domain is responsible for the spectral differences in the 250-nm region. In contrast, the spectrum of RCAM-HPRG, shown for comparison (Figure 5), is distinctly different and resembles that of a denatured protein (cf. HPRG in 3 M guanidine hydrochloride).

The secondary structure of HPRG domains was also assessed by far-UV CD. The spectrum of the N/C fragment reveals a more regular secondary structure than HPRG, as indicated by the presence of a positive peak at 192 nm and the red shift of the negative peak at 205 nm to 208 nm (Figure 6, upper panel), and closely resembles the CD spectrum of fetuin, another member of the cystatin superfamily with a similar domain structure. The spectra of individual HPRG domains (Figure 6, lower panel) reflect their varied primary structures. The large positive peak at 192 nm and the broad negative peak at 208 nm with a shoulder at 220 nm in the CD spectrum of the N-terminal domain is indicative of mainly β-structure with some α-helix content, in agreement with the crystal structure of cystatin (Bode *et al*., 1988) and stefin B (Stubbs *et al*., 1990). Cystatin and stefin B have similar structures, consisting of an α-helix folded against four antiparallel β-sheets, despite their low sequence homology and the lack of disulfide bonds in stefin B. Interestingly, the disulfide bonds of the isolated N-terminal domain of HPRG have been reduced and they do not seem to be necessary to maintain proper folding.

The far-UV CD spectra of both the histidine−proline-rich and the C-terminal domains lack the features of "regular" secondary structure (α-helix or β-sheet), as expected from their high proline content. The single trough at 200 nm in the spectrum of the C-terminal domain is characteristic of random coil structure and is consistent with the higher proportion of "regular" secondary structure in the N-terminal domain as compared with the N/C fragment. Similar spectra have been described for the salivary proline-rich glycoprotein (Loomis *et al*., 1985) and apomucin (Eckhardt *et al*., 1987) and attributed to a high percentage of irregular structure and β-turns.

The CD spectrum of the histidine−proline-rich domain exhibits a large negative peak at 203 nm and a small positive peak at 226 nm, indicative of polyproline(II) helix (Ronish & Krimm, 1974). The influence of calcium chloride on this spectrum confirms this interpretation: the disappearance of the positive peak at 226 nm (see inset in Figure 6) and a reduction in the intensity around 205 nm (not shown) are diagnostic for polyproline(II) helix (Tiffany & Krimm, 1968; Mattice & Mandelkern, 1970). Although the positions of the negative and positive peaks are similar to those seen in the CD spectra of polyhistidine below pH 5 (Myer & Barnard, 1971; Beychok *et al*., 1965) and *Plasmodium* histidine-rich protein (Margossian *et al*., 1990), the intensity of the negative peak around 200 nm in the latter species is much lower than that observed in the spectrum of the histidine−proline-rich domain, which is closer to the values reported for polyproline(II): $-35\,000$ deg·cm^2·dmol^{-1} (Helbeque & Loucheux-Lefebvre, 1982) or $-50\,000$ deg·cm^2·dmol^{-1} (Loomis *et al*., 1991).

To test whether domain preparation has affected the structure of the protein, we tried to simulate the spectra of HPRG and N/C fragment from a linear combination of the spectra of the component domains (Figure 6A). Since errors in determination of the protein concentration can be as large as 10%, we allowed the sum of the coefficients to vary between 90% and 110%. The HPRG spectrum was almost perfectly fitted by a combination of 56% N/C fragment and 34% histidine−proline-rich domain. The expected values based on the domain boundaries indicated in Table 1 would be 77% and 23%, respectively. The higher percent of the histidine−proline-rich domain required in our simulation may be explained by the partial loss of the proline-rich C-terminal portion of the N-terminal domain in our preparation (see above). The best fit for the N/C fragment was obtained by combining 59% N-terminal fragment and 31% C-terminal fragment (74% and 26% expected, respectively). However, the relatively poor fit suggests that the isolation of the N- and C-terminal domains has affected their structure to some degree.

We also tested whether heparin induces any modifications in the secondary structure of HPRG or its domains. Only the CD spectrum of the histidine−proline-rich domain was affected by heparin, indicating interaction between the two species (Figure 6B). However, the changes were confined to the 190−200-nm region and did not lend themselves to a clear-cut interpretation in terms of secondary structure.

Influence of pH on HPRG Structure. Like most serum proteins, HPRG is negatively charged at physiological pH (pI = 6.45; see Table 1). An examination of the amino acid sequence of HPRG reveals that the charged residues are not distributed uniformly. That is, the N/C fragment contains the majority of acidic residues (pI = 5.6−5.8), while the high proportion of histidine (28% on a molar basis) in the histidine−proline-rich peptide (pI = 7.15) raises the isoelectric point of the whole molecule.

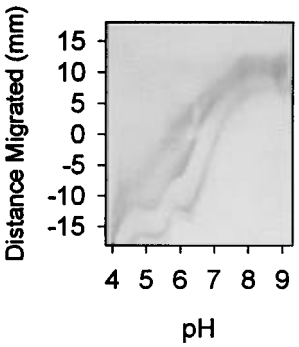

FIGURE 7: Electrophoretic titration curve of HPRG and its domains. A pH gradient was created in a precast IEF 3−9 gel (Pharmacia) by running it for 150 V·h in the first dimension. A mixture of HPRG (middle trace), N/C fragment (upper trace), and histidine−proline-rich fragment (lower trace) was then applied and the gel was run for 40 V·h in the second dimension.

With 34 of 53 total histidine residues, the histidine−proline-rich domain dominates the titration behavior of HPRG in the pH range 5−8. As shown in Figure 7, the electrophoretic titration curve of HPRG more closely resembles that of the histidine−proline-rich domain than that of the N/C fragment. Importantly, the upper range of the HPRG titration curve spans the physiological pH range, although the maximum charge variation with pH, $\delta z/\delta$pH, is found around pH 6.5. The titration curve of the N/C fragment, with an apparent pK_a of 6.0, is relatively broad and shallow, indicating the presence of a heterogeneous mixture of histidine side chains. The titration curve of the histidine−proline-rich domain has some interesting characteristics. First, the $\delta z/\delta$pH in the pH range 6.5−7.0 is about 25 charges/pH unit, about 50% higher than the value obtained from a simulated titration curve, suggesting cooperative protonation. Second, the apparent pK_a value of 7.0 is significantly higher than that expected for unperturbed histidine side chains, implying environmental effects on the pK_a, and making this domain notably sensitive to pH changes in the physiological range. Third, a discontinuity in the titration curve around pH 6.0 suggests, at first sight, the presence of two classes of histidine side chains with apparent pK_a values of 5.8 and 7.0, respectively. However, two classes of residues differing in pK_a by only 1 pH unit would give rise to a smoother titration curve; therefore, the discontinuity observed is likely due to a conformational change that alters the electrophoretic mobility of the histidine−proline-rich domain—either by increasing the frictional coefficient or decreasing the positive charge.

The sedimentation coefficient of HPRG does not change between pH 5.5 and 7.5, nor does the far-UV CD spectrum, suggesting that the secondary structure and the overall shape of the molecule are not significantly affected in this range. However, the sedimentation coefficient of the histidine−proline-rich domain decreases upon acidification, from 1.530 [1.526, 1.532] S at pH 7.2, to 1.488 [1.485, 1.490] S at pH 6.3 and 1.44 [1.436, 1.440] S at pH 5.5, a 6% change overall. The values in brackets represent the 95% confidence intervals, indicating that the observed differences are statistically significant. Since $s = M(1 - \bar{v}\rho)/Nf$ (where all the

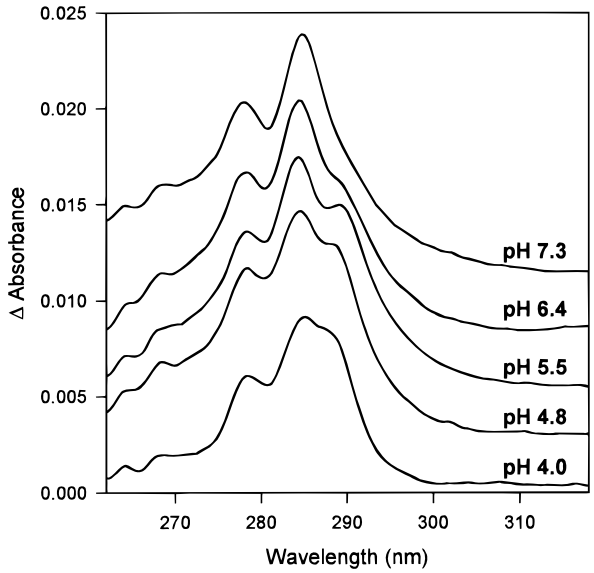

FIGURE 8: Effect of pH on the solvent-perturbation difference spectra of HPRG. HPRG solutions (20 μM) were perturbed with 20% DMSO in tandem cuvettes with a total optical path of 0.876 cm. The buffer was 50 mM sodium phosphate (above pH 5.4) or acetate (below pH 5.4) containing 100 mM sodium chloride. The difference spectra obtained at the various pH values were displaced by 0.0025 Å along the vertical axis to avoid overlap.

terms have their usual meaning) and $\bar{v}$ is little influenced by pH in this range, the changes in *s* should be due to an increase in the frictional coefficient, *f*, in agreement with the titration data. This may be caused, for instance, by the mutual repulsion of protonated histidine side chains and the subsequent increase in the axial ratio. The secondary structure of the histidine−proline-rich domain is minimally affected by acidification in the same pH interval, since the only change in the far-UV CD spectra is a red shift of about 0.5 nm.

Solvent-perturbation difference spectroscopy of HPRG revealed a pH-dependent modification in the exposure of aromatic amino acids (Figure 8). Above pH 7, the difference spectrum is dominated by peaks at 279 and 284 nm, indicating exposure solely of tyrosine (Herskovits, 1967). Lowering the pH causes the appearance first of a shoulder, then of a peak, at 289−290 nm, indicating increasing tryptophan exposure. Similar results were obtained using 20% DMSO or 20% ethylene glycol as perturbant.

An analysis by second-derivative spectroscopy of HPRG spectra taken at various pH values also reveals pH-dependent modifications in the intensity of the peaks above 280 nm (Figure 9, panel A). The changes affect both minima characteristic of tryptophan, *i.e.*, at 286 and 292 nm, but not the tyrosine-specific minimum at 279 nm. Even though tyrosine does contribute to the 286-nm minimum, overall the data are consistent with pH-induced changes in the polarity of the environment of tryptophan. Certain derivatives of HPRG were also studied. Although the N/C fragment contains the full complement of tyrosine and tryptophan residues of HPRG, no pH-dependent changes were observed in the second-derivative spectra of this fragment or in those of partially reduced HPRG. However, the behavior of the plasmin-clipped HPRG is similar to that of the native protein.

To analyze this transition, the peak-to-peak distance between the maximum at 289.5 nm and the minimum at 292

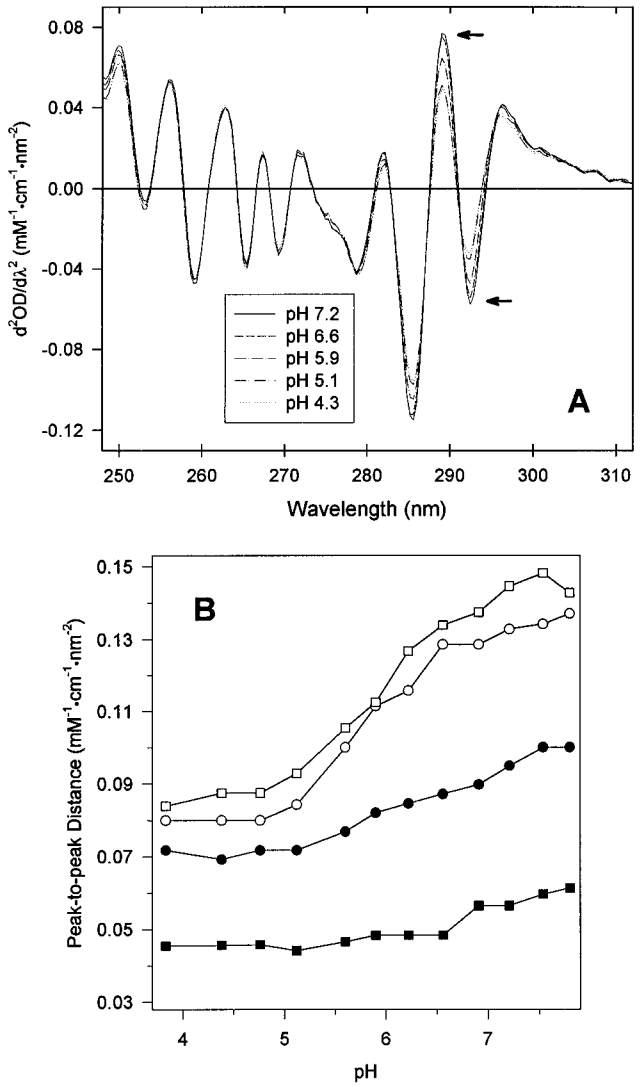

FIGURE 9: Effect of pH on the near-UV absorption spectra of HPRG. Panel *A*: Second-derivative UV spectra of HPRG obtained at the pH values indicated in the inset are shown. The buffer was 50 mM sodium phosphate (above pH 5.4) or acetate (below pH 5.4) containing 100 mM sodium chloride. The peaks at 289 and 292 nm, which exhibit the largest changes with pH, are marked with arrows. Panel *B*: Effect of pH on the 289−292-nm peak-to-peak distance in the second-derivative spectra is shown for HPRG (○), plasmin-clipped HPRG (□), PRCM-HPRG (●), and N/C fragment (■).

nm in the second-derivative spectrum was plotted versus pH (Figure 9, panel B). The transition agrees well with the titration curve of a species with a pK_a of 6.0, consistent with the protonation of one or more histidine residues. The range of the transition corresponds to the discontinuity seen in the electrophoretic titration curves of the histidine−proline-rich domain and HPRG (Figure 7), suggesting that the two phenomena are related.

DISCUSSION

Since only exposed regions in a protein are usually attacked, limited proteolytic digestion often yields intact structural domains. Rabbit HPRG domains have been previously obtained by reverse-phase HPLC (Morgan, 1985), but only limited quantities were available for structural characterization. The stepwise purification protocol described here allows isolation of larger amounts of functional domains under less denaturing conditions. It is interesting

to note that the bias in the amino acid composition of HPRG is reflected in the nature of the fragments produced. Reduction of plasmin-clipped HPRG under nondenaturing conditions releases only the characteristic histidine−proline-rich peptide, leaving the N- and C-terminal domains disulfide linked. This so-called N/C fragment exhibits the features common to other members of the crystatin superfamily, such as α_2HS glycoprotein or HMW-kininogen: *i.e.*, a series of cystatin-like modules at the amino-terminal end, a proline-rich domain at the carboxyl-terminal end, and a disulfide bond linking the first and the last cysteine in the molecule. Little is yet known about the binding properties of the N/C fragment; however, a 40-kDa N-terminal fragment of mouse HPRG decreased macrophage Fc-γ receptor expression and phagocytosis (Chang *et al.*, 1994), and preliminary data showed that the C-terminal domain of rabbit HPRG, in particular the C-terminal lysine, is important for the interaction with plasminogen (Borza & Morgan, 1994).

The histidine−proline-rich domain of HPRG has no close homologs, although a very limited similarity to the histidine-rich domain of heavy kininogen has been noted (Koide *et al.*, 1986), but its function may be easier to approach since it is smaller and has a relatively simple sequence. Of the three HPRG domains, the histidine−proline-rich domain alone qualifies as a "low-complexity" region, as defined in Wootton (1994); such sequences are usually hydrophilic, relatively mobile, and "more likely to generate relatively extended coiled or helical structures". The lack of hydrophobic amino acids in this domain indeed precludes the formation of a compact, globular structure, and its far-UV CD spectrum suggests the presence of polyproline(II) helix, as expected from the high content of proline. The tandem pentapeptide repeats, and especially the presence of glycine every fifth residue—reflecting a requirement for unusual ϕ, ψ angles or sterical constraints—hint at a repetitive structure. A possible structure consistent with the sequence and the properties of the histidine−proline-rich domain is the polyproline/β-turn helix, proposed for the tandem repeat Tyr-Pro-Pro-Gln-Gly from octopus rhodopsin (Matsushima *et al.*, 1990). While the proline and glycine residues in this fragment are expected to confer a structural framework, the histidine residues in the histidine−proline-rich domain are likely to account for its functional properties. For instance, they comprise the multiple binding sites for both heme and divalent transition metal ions (Morgan, 1985), although HPRG does not appear to play a role in serum transport of these ligands under normal physiological conditions.

Changes in the far-UV CD spectrum of the histidine−proline-rich domain upon addition of heparin indicate that these two molecules interact in solution. Previously, we showed that the histidine−proline-rich domain binds to heparin−Sepharose at pH 6.8 but not at pH 7.4, and chemical modification of histidine residues in HPRG abolishes heparin binding (Burch *et al.*, 1987). The neutralization by intact HPRG of the effect of heparin on the thrombin−antithrombin reaction also shows a strong pH dependence in the pH range 7.0−7.4 (Peterson *et al.*, 1987), consistent with histidine involvement in heparin binding. In view of our findings that the histidine−proline-rich domain has a p*I* of 7.15 and its histidine residues have a relatively high pK_a, this domain appears to mediate the pH-sensitive heparin binding, which is dependent on the protonation of histidine side chains. HPRG binds not only to heparin but also to cell-surface heparan sulfate proteoglycans (Brown & Parish, 1994) and to immobilized dermatan sulfate (Zammit & Dawes, 1995). If the binding of HPRG to naturally occurring glycosaminoglycans has a pH dependence similar to that observed for heparin, small pH changes in the physiological range may significantly change the HPRG affinity for glycosaminoglycans and its ability to compete with other glycosaminoglycan-binding proteins (*e.g.*, antithrombin III, acidic or basic fibroblast growth factor, platelet factor 4).

In this paper, we also present evidence for pH-dependent structural changes in HPRG that take place around pH 6.0 and cause increased exposure to solvent of tryptophan residues. These changes are abolished by removal of the histidine−proline-rich domain or by mild reduction with DTT, which cleaves the disulfide bond between the histidine−proline-rich domain and the rest of the molecule (the crystal structure of cystatin suggests that the intradomain disulfide bonds in the cystatin modules of HPRG are buried in the hydrophobic core and the disulfide bond between the N- and C-terminal domains is not reduced under nondenaturing conditions). Thus, local interactions between neighboring amino acids are not sufficient to cause the observed spectral changes, which require an intact disulfide bond between Cys-185 and Cys-407, suggesting the involvement of the histidine−proline-rich domain. Interestingly, this disulfide bond is unique to HPRG and replaces an intradomain disulfide that is conserved among other members of the cystatin superfamily. Together with the electrophoretic and sedimentation behavior of the histidine−proline-rich domain, our data indicate that below pH 6 the protonation of histidine side chains in the histidine−proline-rich domain causes a conformational change that is transmitted through the disulfide bond to the N/C fragment, eventually affecting the environment of tryptophan residues in the latter fragment.

In conclusion, three domains of rabbit HPRG were purified and characterized. The modular architecture of HPRG suggests that it may have several independent binding sites and that its biological role may be to bring two or more ligands together. The unique histidine−proline-rich region may act as a pH sensor and regulate the biological function of HPRG. Small changes in pH may modulate the activity of HPRG by triggering a conformational change as well as by increasing the affinity for negatively charged polymers, such as heparin and glycosaminoglycans. Experiments to clarify the physiological role of this pH-sensitive behavior and to map the binding sites of other HPRG ligands are in progress.

REFERENCES

Beychok, S., Pflumm, M. N., & Lehman, J. E. (1965) *J. Am. Chem. Soc. 87*, 3990−3991.

Biggin, M. D., Gibson, T. J., & Hong, G. F. (1983) *Proc. Natl. Acad. Sci. U.S.A. 80*, 3963−3965.

Bode, W., Engh, R., Musil, D., Thiele, U., Huber, R., Karshikov, A., Brzin, J., Kos, J., & Turk, V. (1988) *EMBO. J. 7*, 2593−2599.

Borza, D. B., & Morgan, W. T. (1994) *FASEB J. 8*, A1295 (abstr).

Brown, K. J., & Parish, C. R. (1994) *Biochemistry 33*, 13918−13927.

Burch, M. K., Blackburn, M. N., & Morgan, W. T. (1987) *Biochemistry 26*, 7477−7482.

Castellino, F. J., & Powell, J. R. (1981) *Methods Enzymol. 80*, 365.

Chang, N. S., Leu, R. W., Rummage, J. A., Anderson, J. K., & Mole, J. E. (1992a) *Immunology 77*, 532−538.

Chang, N. S., Leu, R. W., Rummage, J. A., Anderson, J. K., & Mole, J. E. (1992b) *Blood 79*, 2973−2980.
Chang, N. S., Leu, R. W., Anderson, J. K., & Mole, J. E. (1994) *Immunology 81*, 296−302.
Donovan, J. W. (1973) *Methods Enzymol. 27*, 525−548.
Eckhardt, A. E., Timpte, C. S., Abernethy, J. L., Toumadje, A., Johnson, W. C., & Hill, R. L. (1987) *J. Biol. Chem. 262*, 11339−11344.
Hansen, J. E., Lund, O., Engelbrecht, J., Bohr, H., Nielsen, J. O., & Brunak, C. S. (1995) *Biochem. J. 308*, 801−813.
Helbeque, N., & Loucheux-Lefebvre, M. H. (1982) *Int. J. Pept. Protein Res. 19*, 94−101.
Herskovits, T. T. (1967) *Methods Enzymol. 11*, 748−775.
Koide, T., & Odani, S. (1987) *FEBS Lett. 216*, 17−21.
Koide, T., Foster, D., Yoshitake, S., & Davie, E. W. (1986) *Biochemistry 25*, 2220−2225.
Laemmli, U. K. (1970) *Nature (London) 227*, 680−685.
Laue, T. M., Shah, B. D., Ridgeway, T. M., & Pelletier, S. L. (1992) in *Analytical ultracentrifugation in biochemistry and polymer science* (Harding, S. E., Rowe, A. J., & Horton, J. C., Eds.) pp 90−125, The Royal Society of Chemistry, Cambridge, England.
Leung, L. L., Nachman, R. L., & Harpel, P. C. (1984) *J. Clin. Invest. 73*, 5−12.
Lijnen, H. R., Hoylaerts, M., & Collen, D. (1980) *J. Biol. Chem. 255*, 10214−10222.
Lijnen, H. R., Hoylaerts, M., & Collen, D. (1983) *J. Biol. Chem. 258*, 3803−3808.
Loomis, R. E., Bergey, E. J., Levine, M. J., & Tabak, L. A. (1985) *Int. J. Pept. Protein Res. 26*, 621−629.
Loomis, R. E., Gonzalez, M., & Loomis, P. M. (1991) *Int. J. Pept. Protein Res. 38*, 428−439.
Margossian, S. S., McPhie, P., Howard, R. J., Coligan, J. E., & Slayter, H. S. (1990) *Biochim. Biophys. Acta 1038*, 330−337.
Matsushima, N., Creutz, C. E., & Kretsinger, R. H. (1990) *Proteins: Struct., Funct., Genet. 7*, 125−155.
Mattice, W. L. & Mandelkern, L. (1970) *Biochemistry 9*, 1049−1058.
Miles, E. W. (1977) *Methods Enzymol. 47*, 431−442.
Morgan, W. T. (1978) *Biochim. Biophys. Acta 535*, 319−333.
Morgan, W. T. (1985) *Biochemistry 24*, 1496−1501.
Morgan, W. T., Deaciuc, V., & Riehm, J. P. (1989) *J. Mol. Recog. 2*, 122−126.
Morgan, W. T., Muster, P., Tatum, F. M., Kao, S., Alam, J., & Smith, A. (1993) *J. Biol. Chem. 268*, 6256−6262.
Myer, Y. P., & Barnard, E. A. (1971) *Arch. Biochem. Biophys. 143*, 116−122.
Peterson, C. B., Morgan, W. T., & Blackburn, M. N. (1987) *J. Biol. Chem. 262*, 7567−7574.
Philo, J. (1994) in *Modern Analytical Ultracentrifugation* (Schuster, T. M., & Laue, T. M. Eds.) pp 156−170, Birkhauser, Boston, MA.
Ronish, E. W., & Krimm, S. (1974) *Biopolymers 13*, 1635−1651.
Saez, C. T., Jansen, G. J., Smith, A., & Morgan, W. T. (1995) *Biochemistry 34*, 2496−2503.
Saigo, K., Shatsky, M., Levitt, L. J., & Leung, L. K. (1989) *J. Biol. Chem. 264*, 8249−8253.
Sambrook, J., Fritsch, E. F., & Maniatis, T. (1989) in *Molecular Cloning: a laboratory manual* (Ford, N., Nolan, C., & Ferguson, M., Eds.) pp 118−120, Cold Spring Harbor Laboratory Press, Cold Spring Harbor, NY.
Sanger, F., Coulson, A. R., Barrell, B. G., Smith, A. J. H., & Roe, B. A. (1980) *J. Mol. Biol. 143*, 161−178.
Sorensen, C. B., Krogh-Pedersen, H., & Petersen, T. E. (1993) *FEBS Lett. 328*, 285−290.
Struhl, K. (1985) *Biotechnology 3*, 452−453.
Stubbs, M. T., Laber, B., Bode, W., Huber, R., Jerala, R., Lenarcic, B., & Turk, V. (1990) *EMBO J. 9*, 1939−1947.
Tiffany, M. L., & Krimm, S. (1968) *Biopolymers 6*, 1767−1770.
Wootton, J. C. (1994) *Curr. Opin. Struct. Biol. 4*, 413−421.
Zammit, A., & Dawes, J. (1995) *Blood 85*, 720−726.

BI952061T